3D Printed vs. Traditional Finger Orthoses: A Force Comparison

Clarisse HUMBERT¹, Renaud NICOD¹, Thomas LAMARTINE¹, Arthur CARTERON¹, Sébastien EUPHRASIE^{1,2}, François LOISEL³

1 Université Marie et Louis Pasteur, ISIFC, Biotika, 51 avenue de l'Observatoire, F-25000 Besançon, France

2 Université Marie et Louis Pasteur, CNRS, Institut FEMTO-ST, 15B Avenue des Montboucons, F-25000 Besançon, France

3 Service de Chirurgie Orthopédique et Traumatologique, Plastique et Reconstructrice, SOS Mains, Hôpital Universitaire de Besançon Université Marie et Louis Pasteur, CHU Besançon, SINERGIES (UR 4662), F-25000 Besançon, France

Corresponding author: Sébastien EUPHRASIE

Mail: sebastien.euphrasie@femto-st.fr

Phone: 33-3-63-08-24-34

Contributions:

CH: methodology, software, validation, investigation, Writing - Original Draft

RN: methodology, software, validation, investigation, Writing - Original Draft

TL: methodology, software, validation, investigation, Writing - Original Draft

AC: Resources

SE: Supervision, Writing - Review & Editing

FL: Conceptualization Writing - Review & Editing

Acknowledgments

The authors would like to thank the various students who previously worked on the Orthez3D project at Biotika: Naïs Dewasnes, Juliette Jacquot, Isabel Jaffar, Alan Jost, Laura Genevois, Estelle Giambelluco, Clotilde Has, Carla Lenero, Maïlys Payen

3D Printed vs. Traditional Finger Orthoses: A Force Comparison

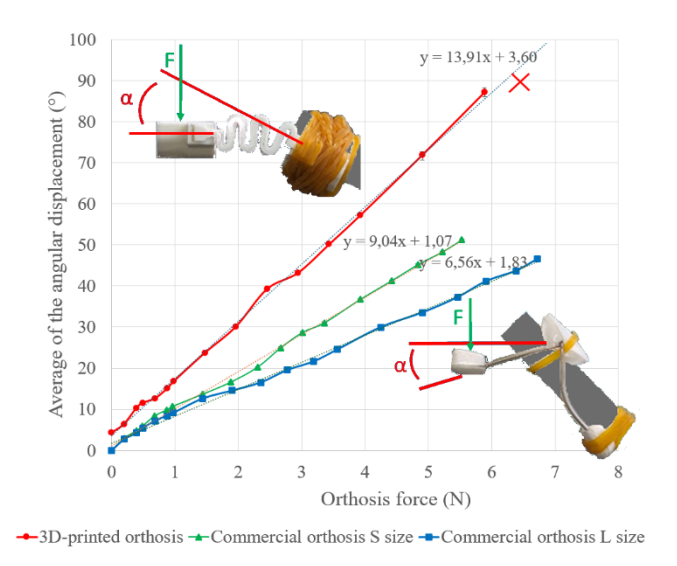
Abstract

Dynamic flexion or extension orthoses for the proximal interphalangeal joint (PIP) are commonly employed in rehabilitation to enhance mobility after trauma. This study aims to compare the biomechanical performance of two commercial extension orthoses (sizes S and L) and a 3D-printed orthosis.

The tests were conducted with increasing loads ranging from 0 g to 1500 g. Angular displacements were measured using a specific experimental setup. The forces exerted were modeled using simplified assumptions about the geometry of the orthoses and their interaction with the finger.

The results show that the 3D-printed orthosis, while offering advantages in customization, exhibited limited mechanical resistance, failing under a load of 700 g. In contrast, the commercial orthoses demonstrated excellent fatigue resistance, with an average angular displacement difference of less than 0.1° between repeated series. The 3D-printed orthosis exhibited the highest slope in the stress-strain curve (13.9 °N⁻¹ compared to 9.3°N⁻¹ and 7°N⁻¹ for commercial S size and L size respectively). These results indicate that, although of the same order of magnitude, this 3D-printed orthosis is more deformable.

In conclusion, commercial orthoses provide better mechanical reliability under the tested conditions, while the 3D-printed orthosis requires improvements. Integrating multi-material components and force sensors could improve durability and efficiency, opening promising perspectives for customized rehabilitation orthoses.



Keywords: digital orthosis, 3D printing, PIP, rehabilitation, biomechanics

1. Introduction

After a trauma (sprain, dislocation) of the proximal interphalangeal (PIP) joint, the main risk is the occurrence of stiffness. Rehabilitation is crucial to restore the function of the injured fingers, and there are many complementary methods. In cases of extension stiffness of the finger or the treatment of a boutonnière deformity, the use of dynamic extension orthoses is a common approach to guide rehabilitation. These orthoses allow for a controlled and progressive flexion movement of the joint, thus helping to prevent stiffness and improve joint mobility [1-3].

Although the market offers a wide range of commercial orthoses, varying in dimensions and design [4], inadequate fitting to the patients' morphology can limit their effectiveness, cause discomfort, and lead to side effects such as excessive pressure or skin irritation [5]. To address these issues, 3D printing has emerged as a promising solution for finger orthosis [1-2, 6-7] or for orthopedics in general [8-11]. This technology enables precise customization of devices, allowing precise adaptation to the patient's anatomy. Recent studies have emphasized the significance of biomechanical measurements in the design of "patient-specific" orthoses [12].

Despite the widespread use of orthoses, precise data on the forces they exert during rehabilitation remain scarce [2]. Yet, understanding these forces is essential to ensure both

therapeutic effectiveness and patient safety. Although no formal consensus exists, empirical recommendations suggest that dynamic orthoses should exert forces between 100 g and 300 g to be both effective and safe [2]. This justifies our biomechanical modeling approach, aimed at quantifying and comparing the mechanical behavior of two different orthosis designs under load. We chose to compare a standard commercial dynamic orthosis with a 3D-printed model, as the latter offers promising advantages in terms of customization and accessibility. However, its mechanical performance remains insufficiently validated. This comparison allows us to assess whether a 3D-printed orthosis can replicate the biomechanical behavior of commercial devices and to identify some technical challenges that must be addressed before clinical application.

Our main objective is to measure and compare the forces exerted on commercially available dynamic extension orthoses and those created through 3D printing for the rehabilitation of the proximal interphalangeal joint. Our hypothesis is that both types of orthoses could demonstrate comparable biomechanical performance under similar loading conditions, despite differences in materials and design. Beyond testing this hypothesis, the study also aims to provide valuable experimental data on both commercial and 3D-printed orthoses, thereby laying the groundwork for future improvements and developments in 3D-printed designs.

2. Material & methods

2.1. Orthoses

The commercial orthoses used were of two different sizes of the Rolyan Sof-Stretch Extension Splint model (Performance Health, 13 Rue André Pingat, 51100 Reims, France): one size S (Fig. 1.a) and one size L. These orthoses consisted of metal rods with polystyrene contact areas to reduce discomfort. They are the only one available in the hospital associated with this study.

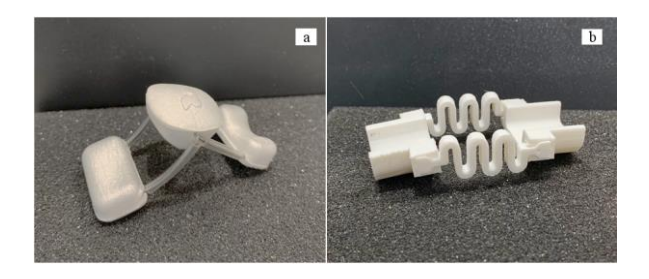


Fig. 1. Photograph of the orthoses. (a) Commercial orthosis (Rolyan Sof-Stretch Extension Splint model, S size). (b) 3D-printed orthosis made of PLA.

The concept behind the design of the 3D-printed orthosis is to enable the fabrication of customized orthoses (in terms of size and applied forces) using only the printed components. The original modeling of this 3D printed orthosis was developed during previous work conducted by master's students within in an academic setting. Several spring designs were tested; the orthosis shown in Figure 1b was selected as a compromise between compact size (ensuring patient comfort), spring constant, and robustness. It was modeled using the computer-aided design software Creo (PTC, 121 Seaport Blvd, Boston, MA 02210, USA). The printing was performed with an Ultimaker 3 printer (Ultimaker BV, Watermolenweg 2, 4191 PN Geldermalsen, Netherlands), the only one available at the time. The printing parameters included the use of Ultimaker PLA (Polylactic Acid) as the material, providing a balance between flexibility and durability, an AA type printer core with a 0.4 mm nozzle, a resolution of 0.15 mm, and an infill of 80%. The printing time was about 2 hours.

2.2. Experimental Set-up and method

2.2.1. Experimental Setup

The experimental setup used to measure the angular displacement of the orthoses under load is presented in Figure 2. It included a clamping system with a bench vise mounted on a swivel. The clamp held an inclined cylinder to simulate the angle of force application. The orthoses were attached to the cylinder using elastic bands. At their distal end, calibrated weights (KERN & Sohn GmbH, Ziegelei 1, 72336 Balingen, Germany) were applied using polyamide threads.

The mass of the threads was neglected in the analysis. The angular displacement was measured using a 360° protractor whose center was aligned with the center of rotation of the orthosis to facilitate measurements. This protractor was held in place by two clamps measuring 10 and 15 cm. A camera mounted on a Cullmann Alpha 2500 Silver tripod (Cullmann Germany GmbH, Gutenbergring 61, 91096 Möhrendorf, Germany) was used to record the movements. The data were analyzed with the Angulus software (V-21 Software, Rue de l'Industrie 58, 1950 Sion, Switzerland) with an accuracy of 0.1°.



Fig. 2. Experimental set-up for angular displacement measurement for commercial orthoses. The main parts are a smartphone for image recording, a clamping system with a bench vise mounted on a swivel, a tube to fix the orthosis and a protractor.

This study was conducted to evaluate the force exerted by dynamic flexion orthoses on the proximal interphalangeal joint (PIP). In this protocol, one or more weights were applied to achieve a total load ranging from 0 g to 1500 g on the distal part of the commercial orthoses and the 3D-printed orthosis. The orthosis was secured with a clamp to ensure accurate alignment at 0° relative to the ground reference, which was verified using a spirit level. For each weight, the procedure was repeated three times: applying the weight, measuring the angle of displacement, and then removing the weight to analyze the repeatability of the measurements. Subsequently, two additional series were conducted, each ranging again from 0 g to 1500 g, in order to study the fatigue resistance of the devices.

2.2.2. Measurement Protocol

For the commercial orthoses, the cylinder was tilted at 45°, allowing the distal part to be horizontal without the addition of weight. The angular displacement was measured using the Angulus app and a protractor. The 0° angle corresponded to the initial position without weight (Fig. 3.a, Fig. 3.b).

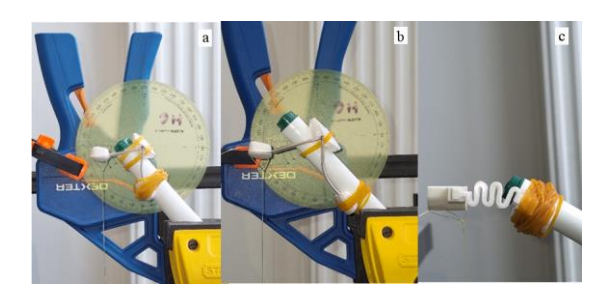


Fig. 3. Examples of angular displacement measurement of the distal part of the orthoses under a load of 200g. (a) Commercial orthosis size S (6.4 cm in length between the distal and proximal parts). (b) Commercial orthosis size L (8.9 cm). (c) 3D-printed orthosis. The initial position is distal part horizontal for (a) and (b). Initial position for (c) is adjusted such that the final position of the distal part is horizontal.

For the 3D-printed orthosis, lacking a defined axis of rotation, a manual adjustment of the cylinder's inclination was necessary to ensure that the distal part of the orthosis remained perpendicular to the wire connected to the weight. This was not necessary in the case of the commercial orthosis, as the equivalent perpendicular load can be derived by multiplying the applied force by a cosine of the angle (see Force Modeling section). The angular displacement was measured with the Angulus app (Fig. 3.c), by measuring the angle between the distal and proximal parts of the orthosis.

The measurement of angular displacement through image processing on Angulus was performed in real-time, resulting in a time interval of 1 to 3 minutes between measurements. The angular uncertainty resulting from the selection of points required for the application is

estimated at 0.2° . For certain masses, several operators were tested, and the resulting values were similar within the $\pm 0.2^{\circ}$ uncertainty.

2.2.3. Force Modeling

The commercial orthoses have a rotation axis located at their medial part. The addition of a weight attached to the distal end resulted in a rotation of an angle α . By reciprocity, the force exerted by the orthoses on the mass corresponded to the opposite of the applied weight. The moment M_0 generated by this force is given by:

$$M_0 = m_1 \times g \times L \times \cos(\alpha)$$
 (1), where

- M₀ is the moment generated by this force
- m₁ was the suspended mass,
- g the gravitational acceleration (9.81 m/s²),
- L the length of the lever arm defined as the distance between the medial and distal parts of the orthosis,
- and α the angle after loading measured between the direction of the applied force and the normal to the lever arm (without weight, the lever arm is horizontal and α is zero).

Now, let's consider the force that the orthosis would exert on a finger when it is deformed by this angle α . By considering the patient's finger as a rigid and incompressible cylinder and the orthosis as a hollow cylinder (splint), their connection can be likened to a sliding pivot. This simplification does not account for the deformation of the finger resulting from tissue softness, for instance. Additionally, potential frictional and shear forces are not considered. Nevertheless, the model offers valuable insights into the overall mechanics. Except for very small loads, finger deformation will have a negligible impact on the measured angle; the angular uncertainty (in radians) is of the order of the deformation divided by the lever arm. The forces that affect the angle are perpendicular, therefore frictional and shear forces should have negligible influence. From a clinical perspective, this simplification means that our results are

representative of the overall mechanical behavior of the orthoses rather than of the exact force distribution on soft tissues. While this limits the precision of direct translation to patient-specific conditions, it provides a reliable comparative framework to evaluate different orthosis designs under controlled conditions. The force exerted by the orthosis on the finger is thus perpendicular to the lever arm (Fig. 4). Since the angle α is the same, its moment is the same as when the weight is applied. Therefore, the force F_1 exerted by the orthosis on the finger would be:

$$F_1 = M_0/L = m_1(\alpha) \times g \times \cos(\alpha)$$
 (2), where

- F₁ is the force exerted by the orthosis on the finger,
- M₀ is the moment generated by this force
- L the length of the lever arm defined as the distance between the medial and distal parts of the orthosis,
- m₁ was the suspended mass,
- g the gravitational acceleration (9.81 m/s²),
- α the angle after loading measured between the direction of the applied force and the normal to the lever arm (without weight, the lever arm is horizontal and α is zero).
- $m_1(\alpha)$ is the mass inducing an angular deformation α .

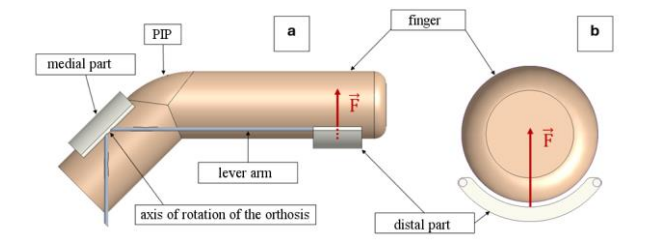


Fig. 4. Diagram of the force exerted by a commercial orthosis on the finger. (a) Side view. (b) Front view.

In the case of the 3D-printed orthosis, the force due to the weight of the added mass m₂ was applied perpendicularly to the distal part of the orthosis. Thus, the force F2 exerted by the orthosis on a finger can be expressed by the following relation:

$$F_2 = m_2(\alpha) \times g$$
 (3), where

- α is the variation of the angle of the distal part before and after applying the load,
- $m_2(\alpha)$ corresponds to the mass that induced the angular deformation α
- and g the gravitational acceleration (9.81 m/s²).

The curves in Figures 5 (average angle α as a function of mass) and 6 (average angle α as a function of the force of the orthosis on the finger) were created using Microsoft Excel software (Microsoft Corporation, One Microsoft Way, Redmond, WA 98052-6399, USA). The standard deviations as well as the linear regressions were also calculated with this software. The errors bars corresponding of the maximum and minimum values are hardly visible since their length is of the same order as the markers used for the data points.

3. Results

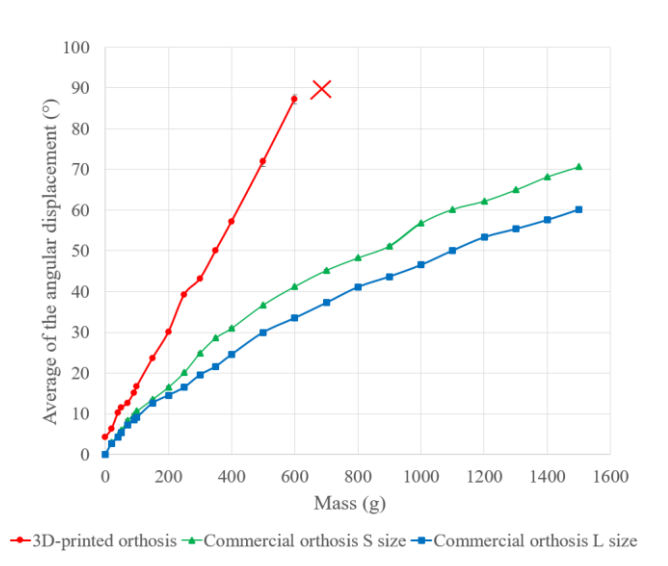


Fig. 5. Average angular displacement as a function of applied mass for the three orthosis models (3D-printed, commercial S size, commercial L size). Error bars (minimum–maximum) are included but hardly visible as their size is of the same order as the data symbols. A red cross indicates the failure point of the 3D-printed orthosis

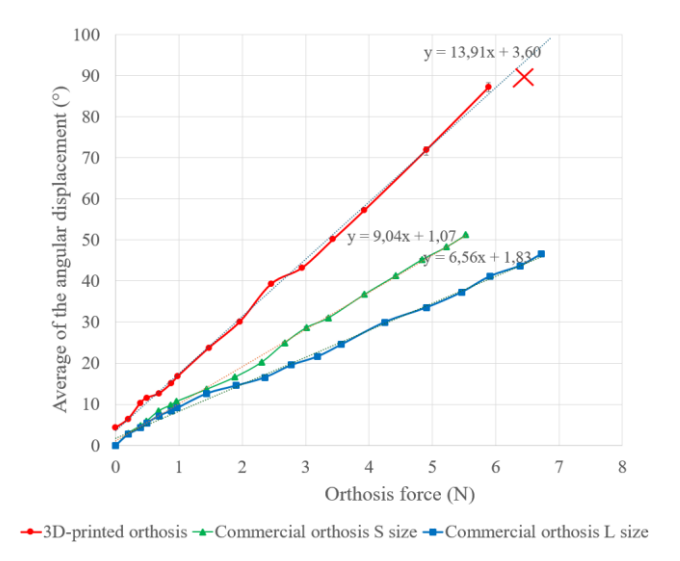


Fig. 6. Average angular displacement as a function of estimated force exerted by each orthosis on a finger (3D-printed, commercial S size, commercial L size). Error bars (minimum—maximum) are included but hardly visible as their size is of the same order as the data symbols. Linear fits are also shown with their regression equations.

	mean angle ± standard deviation			
Mass(g)	3D-printed	S-size	L-size	
0	4.27 ± 0.15	0.00 ± 0.00	0.00 ± 0.00	
20	6.37 ± 0.06	2.94 ± 0.05	2.70 ± 0.10	
40	10.30 ± 0.10	4.74 ± 0.09	4.30 ± 0.12	
50	11.53 ± 0.06	5.92 ± 0.04	5.46 ± 0.05	
70	12.63 ± 0.15	8.40 ± 0.07	7.24 ± 0.15	
90	15.10 ± 0.10	9.86 ± 0.05	8.42 ± 0.13	
100	16.77 ± 0.06	10.70 ± 0.07	9.08 ± 0.13	
150	23.70 ± 0.17	13.60 ± 0.07	12.54 ± 0.15	
200	30.10 ± 0.20	16.58 ± 0.04	14.64 ± 0.23	
250	39.23 ± 0.23	20.26 ± 0.05	16.52 ± 0.08	
300	43.20 ± 0.10	24.96 ± 0.05	19.50 ± 0.14	
350	50.13 ± 0.06	28.70 ± 0.07	21.68 ± 0.16	
400	57.20 ± 0.20	31.12 ± 0.11	24.68 ± 0.16	
500	71.93 ± 1.08	36.82 ± 0.13	29.94 ± 0.15	
600	87.20 ± 1.10	41.32 ± 0.08	33.58 ± 0.16	
700	break	45.22 ± 0.04	37.30 ± 0.07	
800		48.30 ± 0.07	41.18 ± 0.13	
900		51.24 ± 0.05	43.70 ± 0.10	

1000	56.78 ± 0.08	46.74 ± 0.28
1100	60.20 ± 0.07	50.10 ± 0.20
1200	62.20 ± 0.00	53.32 ± 0.13
1300	64.98 ± 0.04	55.40 ± 0.19
1400	68.18 ± 0.04	57.62 ± 0.22
1500	70.62 ± 0.11	60.16 ± 0.13

Table 1. Average of the angular displacement and the standard deviation as a function of the mass of the different orthosis models



Fig. 7. Photography of the 3D-printed orthoses after failure with a weight of 700 g.

	3D-printed orthosis	S-size orthosis	L-size orthosis
lever arm (mm)		25	45
distance between midpoint of the distal segment and anchor in the proximal segment (mm)	40		
maximum tested mass (g)	700 (failure)	1500	1500
larger reached angle (°)	87.2	60.2	50.1
angle-to-force slope (°N ⁻¹)	13.9	9.3	7
fatigue	could not be evaluated	none after 3 tests	none after 3 tests

Table 2. Summary of orthosis specifications and results

Table 1 and figure 5 present the experimental results. It is noteworthy that the maximum flexion of approximately 90° was not reached during these measurements. The 3D-printed orthosis failed when subjected to a load of 700 g. The spring delaminated along some filaments without complete rupture. This delamination did not occur along the layer planes but followed the lines of printing: the delamination plane is orthogonal to the print plane and parallel to the

length of a filament (cf. fig. 7). All measurements show a standard deviation of less than 0.3°, which indicates good reproducibility.

For the two sizes of commercial orthoses, fatigue resistance was assessed using two similar additional series. The quantification of fatigue was obtained by comparing the angular displacement values between the two series. The average difference in angular displacement measurements between the two series is less than 0.1° for both sizes of orthoses, which is at least three times lower than the standard deviation of the measurements.

The angular displacements caused by a patient's finger as a function of the forces exerted by the orthoses are illustrated in Figure 6. For the commercial orthoses, only the overall linear part of the curve has been plotted, along with its linear approximation whose equation is provided alongside. The threshold masses were 900 g for the size S orthosis and 1000 g for the size L orthosis. The 3D-printed orthosis exhibits the steepest slope (13.9 °N⁻¹ compared to 9.3°N⁻¹ and 7°N⁻¹ for commercial S size and L size respectively), indicating greater deformation under a given load. The results also reveal that the slopes of the two commercial models differ: the angular displacement of the size S orthosis is more than 30% greater than that of the size L orthosis for the same applied force. Table 2 summarizes the orthosis specifications (lever arm for the commercial orthoses and the distance between midpoint of the distal segment and anchor in the proximal segment for the 3D-printed orthosis) and main results.

4. Discussions

Our initial hypothesis was that the 3D-printed orthosis could exhibit biomechanical performance comparable to that of commercial models for the proximal interphalangeal (PIP) joint, despite differences in materials and design. However, this hypothesis was not confirmed by our results. Nonetheless, the order of magnitude of the slope angle/load is maintained (13.9 °N⁻¹ compared to 9.3°N⁻¹ and 7°N⁻¹ for commercial S size and L size respectively). Moreover,

the interpolated mass needed to achieve an angle of 80° with the 3D printed orthosis is similar to that of the extension spring described in [2] (560 g versus 433.5 g). By adjusting the dimensions and/or material properties, these values can be modified.

The slope of the force—angle relationship reflects the mechanical stiffness of the orthosis. A steeper slope indicates that less force is required to achieve a given angular displacement, which may be desirable to remain within the empirically recommended range of 100–300 g [2]. From a biomechanical standpoint, the slope also corresponds to the torque delivered by the orthosis to the joint: higher stiffness results in greater resistance to movement, which can facilitate joint correction but may also increase the risk of discomfort or tissue stress. Therefore, an optimal balance is required to ensure both mechanical efficiency and patient safety

The 3D-printed orthosis, due to its customizable nature, can meet the specific needs of each patient. However, its limited mechanical strength, demonstrated by its failure during testing, highlights the challenge of designing an orthosis capable of withstanding the stresses associated with repetitive movements. Since delamination follows the filament path, adjusting the printing parameters may mitigate the problem. Although the maximum angle of 90° was not attained because of the failure, a mass of 600g resulted in an angle of 87.2°. This is sufficient, as such a large angle should not be used in rehabilitation. However, this failure highlights the need for more robust designs, which could be achieved by optimizing printing parameters, exploring alternative materials, or considering multi-material approaches to better balance strength and flexibility. Adjusting the 3D-printer parameters may slightly improve the robustness.

Unlike static 3D-printed orthoses, for which a wide range of robust materials is available, dynamic orthoses require materials that provide an ideal compromise between flexibility, durability, and resistance to mechanical fatigue [14]. This requirement complicates their development, but it is crucial for ensuring effective and safe rehabilitation.

One area for improvement could be the use of other materials. For instance, polyethylene terephthalate glycol (PETG) was found to exhibit greater robustness, offering better flexural resistance [10]. In [9], the authors used thermoplastic polyurethane (TPU) filaments with an active foaming agent, in order to adjust the 3D-printed orthoses' mechanical properties via process parameters such as printing temperature. Using multi-material 3D printing technologies, such as PolyJet printing, would allow for the combination of rigid and flexible materials within a single structure [15]. This facilitates the design of orthoses that combine the necessary mechanical strength and durability with the essential flexibility for patient comfort and mobility, unlike PLA, which is typically a single rigid material. By incorporating specialized flexible materials alongside rigid ones, PolyJet-print orthoses can better withstand daily stresses and deformations, reducing the risk of fracture or failure. In contrast, PLA's inherent brittleness limits its capability to absorb impact or adapt to dynamic loading conditions, potentially compromising the device's longevity and effectiveness. Softer materials in contact with the skin can also improve patient comfort. At this stage of this work, no experimental data are available regarding PolyJet printing; this perspective is based on the anticipated benefits of the technology and will be explored in future studies. They would include comparative tests on different materials such as nylon or composites, would also be necessary to identify the most suitable options for this type of device.

The average angular displacement difference between the two series of commercial orthoses (less than 0.1°) indicates that both models exhibit significant fatigue resistance, with negligible impact of load repetition on mechanical performance. Moreover, the differences in slopes observed between the two sizes of commercial orthoses suggest that, depending on the size, the patient will need to apply different forces to achieve a similar angular displacement. Additionally, contrary to intuition, the larger size orthosis requires greater force to achieve the same angle, resulting in even greater torque (greater force multiplied by a longer lever arm).

While orthosis size is clinically chosen based on finger dimensions, the corresponding variation in mechanical behavior is not systematically calibrated. Since only one orthosis per size has been examined in this study, these findings may be influenced by design variability. Nonetheless, the challenge of precisely controlling the applied force with commercial orthosis poses a risk of inconsistent effects on the rehabilitation treatment. Therefore, adapting orthoses to the patient's morphology is not solely about their size; it must also account for the mechanical and geometric properties of the design. A practical application would be that therapists should consider not only anatomical fit but also mechanical performance when selecting or customizing orthoses. To support this, manufacturers should provide clear information on the biomechanical properties of each model. Moreover, orthosis designs should be adapted to ensure consistent therapeutic effects across different sizes, taking into account individual anatomical variability. In line with these considerations, our results reinforce the importance of prescribing orthoses according to both anatomical adaptation and force calibration, so that the applied load remains within the clinically recommended range for safe and effective rehabilitation.

In addition to biomechanical performance, clinical usability is essential. Recent studies have shown that 3D-printed orthoses can provide comparable functional outcomes with higher patient satisfaction and reduced production time [16-17]. Tobler-Ammann *et al.* [18] further confirmed their feasibility and safety in clinical use, supporting the potential of 3D-printing for patient care once mechanical durability is improved.

An additional strength of this work is the acquisition of data regarding the forces exerted by dynamic orthoses and the theoretical force that a patient's finger would exert on the orthosis. The collected data allow for the quantification of angular displacements under increasing loads and the deduction of the forces applied by the orthoses on the finger. These experimental results also enabled us to model the force that a finger would exert on the orthosis, using simplifying

assumptions such as point forces, finger stiffness, and lever arms defined by the design of commercial orthoses. This data provides a promising foundation for the calibration and optimization of orthoses, particularly in the context of advanced customization for rehabilitation.

The present study has several limitations. First, the sample size was very limited, as only one 3D-printed orthosis and one of each commercial type were tested, which restricts the generalizability of the results. Second, no user trials were conducted, preventing direct assessment of comfort, skin tolerance, and patient adherence. Third, the force calculations relied on a simplified model of the finger as a rigid cylinder, which does not account for soft tissue deformation or friction. In addition to these major limitations, other factors must also be considered: the restriction to a single material (PLA), the absence of long-term fatigue testing, the limited representativeness of the test duration, the potential influence of environmental parameters, and the need for cyclic or dynamic loading protocols. Beyond mechanical considerations, practical issues such as printing time, cost, integration into clinical workflows, and patient comfort should also be addressed before clinical adoption.

5. Conclusion

3D printing offers promising opportunities for the customization of orthotics, thus addressing the specific needs of patients with hand disorders. However, their development requires overcoming several challenges, including robustness to withstand mechanical stresses, comfort to prevent irritation, and ease of use to enhance patient acceptance.

Our study lays the groundwork for developing optimized dynamic orthoses. It emphasizes the importance of continuing research. Implementing a mechanical system, with a step-motor to repeatedly flex the orthoses multiple times would evaluate their mechanical fatigue after predefined milestone flexions. It would also permit to check the dynamical loading behavior. Another potential avenue for progress is, for example, integrating force sensors into 3D-printed

orthoses to enable real-time measurement of applied pressures This approach would provide even more precise calibration, tailored to the needs of each patient, thereby offering concrete avenues for optimizing the design and use of orthoses in rehabilitation.

Conflicts of interest

All other authors declare no conflicts of interest.

One of the author has no conflicts of interest related to this work but is a consultant for Médartis and has other relationships with Evolutis, Kérimédical, Arthrex, and Newclip.

References

- Punsola-Izard V, Schultz KS, Ozaes-Lara E, Mendieta-Zamora J, Romera-Orfila G,
 Carnicero N, Llusá-Perez M, Casado A (2023) Preliminary study of elastic-tension
 digital neoprene orthoses for proximal interphalangeal joint flexion contracture. *Hand*Surgery and Rehabilitation 42 (1): 69-74.
 https://doi.org/10.1016/j.hansur.2022.10.006.
- Fess EE (1988) Force magnitude of commercial spring-coil and spring-wire splints designed to extend the proximal interphalangeal joint. *Journal of Hand Therapy 1(2)*: 86-90. https://doi.org/10.1016/S0894-1130(88)80053-X.
- 3) The Forces of Dynamic Orthotic Positioning: Ten Questions to Ask Before Applying a Dynamic Orthosis to the Hand [Internet]. Musculoskeletal Key. 2019 [consulted 2024 sept 13rd]. https://musculoskeletalkey.com/the-forces-of-dynamic-orthosis-to-the-hand/
- 4) Tourniaire H (2001) Les orthèses dynamiques des interphalangiennes proximales,

 D.I.U Rééducation et appareillage de la main report, Université J. Fourier, Grenoble,

 France https://www.sfrm-gemmsor.fr/file/medtool/webmedtool/gemmtool01/botm0027/pdf00001.pdf

- 5) Saebo. Hand Splints and Contracture: What You Need to Know. [consulted on 2024 sept 17th]. https://www.saebo.com/blogs/clinical-article/hand-splints-contracture-need-know
- 6) Yu, J-T, Huang Y-C, Chen C-S (2024) Research and Development of a 3D-Printed Dynamic Finger Flexion Orthosis for Finger Extension Stiffness—A Preliminary Study. *Bioengineering*, 11(4): 339. https://doi.org/10.3390/bioengineering11040339
- 7) Huber J, Slone S, Bazrgari B (2023) An evaluation of 3D printable elastics for post stroke dynamic hand bracing: a pilot study, *Assistive Technology* 35:6, 513-522. https://doi.org/10.1080/10400435.2023.2177774
- 8) Wong KC (2016) 3D-printed patient-specific applications in orthopedics, *Orthop Res Rev.* 14(8): 57-66. https://doi.org/10.2147/ORR.S99614
- 9) Popescu D, Iacob MC, Tarbă C, Lăptoiu D, Cotruţ C M (2024). Exploring a Novel Material and Approach in 3D-Printed Wrist-Hand Orthoses, *Journal of Manufacturing and Materials Processing* 8(1): 29. https://doi.org/10.3390/jmmp8010029
- 10) Vlăsceanu D, Popescu D, Baciu F, Stochioiu C (2024) Examining the Flexural Behavior of Thermoformed 3D-Printed Wrist-Hand Orthoses: Role of Material, Infill Density, and Wear Conditions, *Polymers* 16(16): 2359. https://doi.org/10.3390/polym16162359
- 11) Reis P, Volpini M, Maia JP, Guimarães IB, Evelise C, Monteiro M, Rubio JCC (2022)

 Resting hand splint model from topology optimization to be produced by additive manufacturing, *Rapid Prototyping Journal* 28(2): 216-225. https://doi-org/10.1108/RPJ-07-2020-0176
- 12) Achouri K. (2021) Développement de dispositifs de mesures biomécaniques pour l'aide à la conception des orthèses articulaires patient-spécifique, PhD thesis from Université Grenoble Alpes. https://theses.hal.science/tel-03352187

- 13) https://angulus-measure-angles-on-images-videos.fr.softonic.com/android
- 14) Umer U, Mian SH, Moiduddin K, Alkhalefah H (2023), Exploring orthosis designs for 3D printing applying the finite element approach: Study of different materials and loading conditions. *Journal of Disability Research*. 2(1):85-97. https://doi.org/10.57197/JDR-2023-0011.
- 15) Li J, Chen S, Shang X et al. (2022), Research Progress of Rehabilitation Orthoses Based on 3D Printing Technology. *Advances in Materials Science and Engineering* https://doi.org/10.1155/2022/5321570
- 16) Oud J *et al.* (2024), Preliminary effectiveness and production time and costs of three-dimensional printed orthoses in chronic hand conditions: an interventional feasibility study. Journal of Rehabilitation Medicine (56). https://doi.org/10.2340/jrm.v56.39946
- 17) Portnoy S. *et al.* (2020) Automated 3D-printed finger orthosis versus manual orthosis preparation by occupational therapy students: Preparation time, product weight, and user satisfaction, *Journal of Hand Therapy* (33): 174-179. https://doi.org/10.1016/j.jht.2020.03.022
- 18) Tobler-Ammann B. *et al.* (2025) Acceptability and safety of 3D printed wrist-based orthoses compared to fiberglass casts for the treatment of non-surgical distal radius- and scaphoid fractures: A randomized feasibility trial. *Journal of Hand Therapy* (38):143-151. https://doi.org/10.1016/j.jht.2024.11.004